

# Evaluating nitrate uptake in a Rocky Mountain stream using labelled $^{15}\text{N}$ and ambient nitrate chemistry

K. A. Hubbard Jr.,<sup>1</sup> L. K. Lautz,<sup>2\*</sup> M. J. Mitchell,<sup>3</sup> B. Mayer<sup>4</sup> and E. R. Hotchkiss<sup>5</sup>

<sup>1</sup> Groundwater & Environmental Services, Inc., 300 Gateway Park Drive, North Syracuse, New York 13212, USA

<sup>2</sup> Department of Earth Science, 204 Heroy Geology Laboratory, Syracuse University, Syracuse, NY 13244, USA

<sup>3</sup> Department of Environmental and Forest Biology, SUNY College of Environmental Science and Forestry, 1 Forestry Drive, Syracuse, NY 13210, USA

<sup>4</sup> Department of Geoscience, University of Calgary, Calgary, AB, T2N 1N4, Canada

<sup>5</sup> Program in Ecology, Department of Zoology and Physiology, University of Wyoming, Laramie, WY 82071-3166, USA

## Abstract:

Background aqueous chemistry and  $^{15}\text{N}_{\text{nitrate}}$  tracer injection methods were used to calculate in-stream nitrate uptake metrics at Red Canyon Creek, a third-order stream in the Rocky Mountains in the state of Wyoming, United States. 'Net' nitrate uptake lengths, which reflect both nitrate uptake and regeneration, and 'gross' nitrate uptake lengths, which exclude re-mineralization, were quantified separately from background nitrate chemistry and  $^{15}\text{N}$  labelling tracer data, respectively. Gross nitrate uptake lengths, from tracer injections of  $^{15}\text{N}$  labelled nitrate, ranged from 502 to 3140 m. Net nitrate uptake lengths, from background nitrate chemistry downstream of a point source, ranged from 1170 to 4330 m. Diurnal changes in uptake lengths suggest the importance of nitrate utilization by autotrophs in the stream and benthic zone. The differences between net and gross nitrate uptake lengths along lower reaches of Red Canyon Creek allowed us to estimate the nitrate regeneration rate, which was  $0.056\text{--}0.080\ \mu\text{mol m}^{-2}\ \text{s}^{-1}$  during the day and  $0.0062\text{--}0.0083\ \mu\text{mol m}^{-2}\ \text{s}^{-1}$  at night. Spatial patterns of streambed pore water chemistry indicate those areas of the hyporheic zone where denitrification was likely occurring. Permanent log dams generated stronger redox gradients in the hyporheic zone than areas with transient beaver dams. By combining isotopically labelled nitrate additions, estimates of uptake from background aqueous nitrate chemistry and characterization of redox conditions in the hyporheic zone, we were able to determine the nitrate regeneration rate and the redox processes responsible for nitrogen cycling in the hyporheic zone. Copyright © 2010 John Wiley & Sons, Ltd.

KEY WORDS nitrogen; uptake length; hyporheic zone; stable isotopes; tracer test; labelled  $^{15}\text{N}$

Received 23 November 2009; Accepted 19 April 2010

## INTRODUCTION

Anthropogenic inputs of nitrogen to the environment are now equal to or exceed those of naturally fixed nitrogen (Galloway and Cowling, 2002; Rockstrom *et al.*, 2009; Schlesinger, 2009). Headwater Rocky Mountain catchments are important areas of study for nitrogen dynamics because high-altitude streams have recently shown increased inorganic N in wet deposition (Fenn *et al.*, 2003a,b; Burns, 2004). Large increases in inorganic N deposition have the potential to shift historically N-limited ecosystems toward N-saturation or reduced N-removal efficiency (Earl *et al.*, 2006; Hall *et al.*, 2009b). The increased export of inorganic N, such as nitrate, due to increased wet deposition in headwater catchments will translate to greater inorganic N in larger rivers (Williams *et al.*, 2001). Headwater streams are crucial sites of nutrient cycling and transport, comprising nearly 85% of total stream length in a given drainage network and serving as collection points of water and dissolved nutrients from terrestrial sources (Peterson *et al.*, 2001). These streams play a disproportionately large role in N

transformation at the landscape scale relative to their small size compared to larger rivers. It has been estimated that nearly 40% of nitrogen chemical species are lost to denitrification in river systems before they can reach the oceans (Seitzinger, 1988; Burns, 1998; Seitzinger *et al.*, 2002). Understanding the complexities of nitrogen cycling in aquatic ecosystems, and particularly headwater streams, is essential in order to predict effects of nitrogen loading on downstream ecosystems (Duff and Triska, 2000).

Nearly all nitrogen transformations (e.g. nitrification and denitrification) occurring in stream ecosystems are controlled by biota (Duff and Triska, 2000). Transformations of nitrogen in the water column include assimilatory uptake and adsorption. Transformations of nitrogen also readily occur in the hyporheic zones of streams due to the variable redox conditions and microbial communities typically present in streambed sediments. Relatively pristine Rocky Mountain streams typically have higher streambed complexity and thus greater hyporheic exchange than those streams that have been physically altered by anthropogenic activities. Hyporheic exchange in mountain streams has caused nitrate demand to be higher than otherwise expected (Hall *et al.*, 2009a). The increased hyporheic storage in the less-disturbed streams

\* Correspondence to: L. K. Lautz, Department of Earth Science, 204 Heroy Geology Laboratory, Syracuse University, Syracuse, NY 13244, USA. E-mail: lklautz@syr.edu

should correspond to greater N removal and transformation in zones of hyporheic exchange or dead zone storage (Gooseff *et al.*, 2007). In order to fully understand the impact of the introduction of anthropogenic nitrogen to Rocky Mountain stream systems, we must first understand the processes that transform and remove nitrogen species from these systems.

In-stream nitrogen addition tracer tests are a tool commonly used to understand nitrogen cycling in stream ecosystems. Nitrogen addition tests have been used to determine nutrient (e.g. nitrate or ammonium) uptake rates and lengths in streams throughout the United States (Mulholland *et al.*, 2002, 2008; Hall *et al.*, 2009b). For example, the Lotic Intersite Nitrogen eXperiment II (LINX II) project, a multi-site study of nitrogen uptake and transformations in different aquatic settings in different geographic regions of the United States has used tracer addition tests with isotopically labelled nitrate to measure nitrate uptake within study reaches (Mulholland *et al.*, 2008). In-stream nutrient cycling can be described using the 'nutrient spiral' concept, which is defined as the total longitudinal distance a nutrient molecule travels as it makes one complete cycle from the dissolved inorganic phase within the water column, through the ecological component of the stream, and back to the dissolved inorganic phase (Newbold *et al.*, 1981; Stream Solute Workshop, 1990; Mulholland and DeAngelis, 2000). A stream's nitrate uptake length ( $S_w$ ) takes into account the additive effects of biological, chemical and physical processes that transform and remove nitrate from water. Sufficiently short in-stream nutrient addition tracer tests (e.g. <24 h) assume re-mineralization of tracer nutrients from the ecological pool is minimal and hence observed loss of the nutrient from stream water is attributed to the various uptake pathways (Payn *et al.*, 2005).

Hydrological factors (e.g. discharge and velocity) and biological factors (e.g. microbial and autotrophic processes) affect nutrient spiralling. Nutrient uptake length is typically shorter in low-order streams due to lower stream velocity that results in longer solute residence time and greater solute contact time with biologically active sediments (Ensign and Doyle, 2006). Headwater streams also tend to have increased water residence time and solute retention due to increased surface-ground water interactions in the hyporheic zone (Valett *et al.*, 1996; Alexander *et al.*, 2000).

In our study, we characterized uptake lengths of nitrate in a small headwater stream in the Rocky Mountains using both  $^{15}\text{N}_{\text{nitrate}}$  addition tracer tests and background nitrate chemistry. We demonstrated how a point source of nitrate can be used to determine 'net' nitrate uptake length, which includes the combined effects of uptake and regeneration processes. We demonstrate how the net uptake length is compared to the more typically reported 'gross' nitrate uptake length, which excludes mineralization and is derived from in-stream isotope addition tests during day and night. We also evaluated the potential for nutrient transformations in the hyporheic zone around

in-stream dams and link nitrate uptake to rates of ecosystem metabolism. The objectives of this study were to: (1) calculate and compare nitrate uptake parameters from background chemistry and isotopic injection methods at the study site and (2) investigate the impact of a man-made dam and beaver dam on hyporheic exchange and subsequent effects on nitrogen cycling.

## SITE DESCRIPTION

The study sites included three reaches within the Red Canyon Creek Watershed, which is located in a semi-arid region of central-western Wyoming, United States (Figure 1). The Red Canyon Creek watershed encompasses 80 km<sup>2</sup>, draining into the Little Popo Agie River approximately 15 km southeast of Lander, Wyoming. Red Canyon Creek is a third-order stream underlain primarily by bedrock consisting of carbonate, siltstone, shale and sandstone (Jin *et al.*, 2010).

Our study area included three reaches with varying morphology and density of in-stream dams (Table I, Figure 1). The furthest upstream experimental reach (Reach C) was located upstream of the confluences of the main stem of Red Canyon Creek with Cherry Creek, the main tributary, and Barrett Creek (Figure 1). The second experimental reach (Reach B) was located immediately downstream of the confluence of Cherry Creek and Red Canyon Creek (Table I, Figure 1). Reach B contained several debris dams, log dams and beaver dams. The third experimental reach (Reach A) (Table I, Figure 1) was located near the outlet of the Red Canyon Creek watershed along a reach that has been the subject of previous research (Lautz and Siegel, 2006, 2007; Lautz *et al.*, 2006). Reach A contained one log dam and one beaver dam, which are locations where we conducted a more detailed investigation of nitrate dynamics in the hyporheic zone.

## METHODS

### *<sup>15</sup>N tracer addition experiments*

A total of three independent  $^{15}\text{NO}_3^-$  addition tracer tests were completed on the three separate study reaches. The  $^{15}\text{NO}_3^-$  addition experiments were done in sequence, starting at the most downstream reach (Reach A) and working upstream in order to ensure that the earlier experimental additions did not affect the later experiments. Each of the  $^{15}\text{NO}_3^-$  addition tests was designed to follow modified LINX II protocols (Mulholland *et al.*, 2008). This study focused on calculating nitrate uptake length ( $S_w$ ) using  $^{15}\text{N}$  tracer injections.

To obtain background nitrate concentrations and nitrogen isotopic ratios in the stream water and groundwater within the three study reaches, pre-addition sampling was conducted 1 h prior to the injection of the isotopic tracer. Pre-addition sampling of groundwater included eight streamside monitoring wells and piezometers in

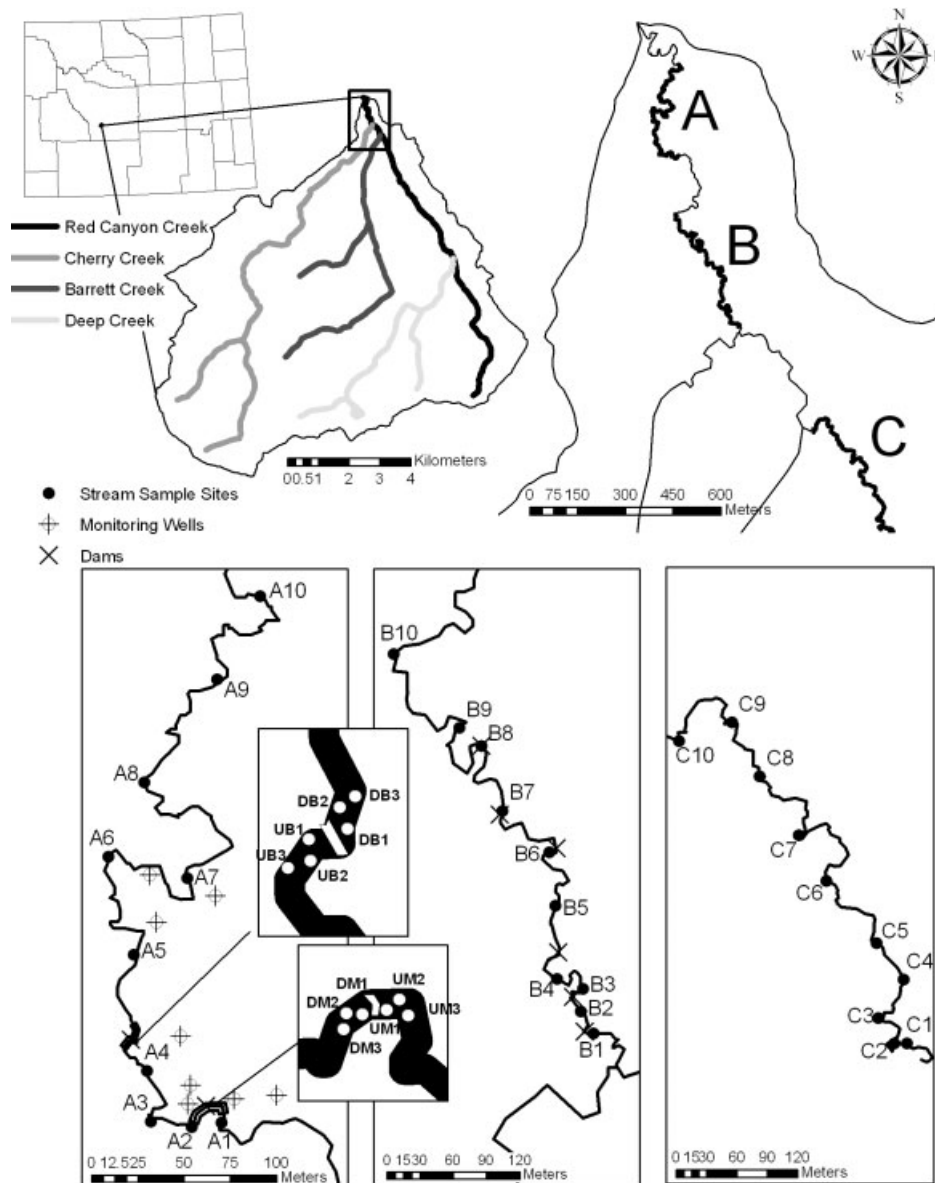


Figure 1. Site map of Red Canyon Creek experimental reaches

the meadow adjacent to Reach A (Figure 1). Along Reach A, the streambeds around a new beaver dam (constructed between August 2007 and June 2008, before the tracer experiments) and a previously studied log dam (constructed in 1993) were instrumented with in-stream mini-piezometers (Figure 1). Six 1.6 cm inner diameter PVC mini-piezometers were installed (three upstream and three downstream) surrounding each dam. The mini-piezometers were screened from 20 to 30 cm below the streambed. To obtain pre-tracer addition water chemistry of the hyporheic zone adjacent to the dams, water samples were collected from each of the mini-piezometers prior to the start of the tracer experiment in Reach A.

During the in-stream tracer tests, a conservative fluorescent dye, Rhodamine Water Tracer (RWT), was co-injected with the isotopically labelled nitrate tracer. Nitrate was co-injected in the form of 98%  $^{15}\text{N}$ -enriched potassium nitrate solution ( $\text{K}^{15}\text{NO}_3$ ), purchased from Sigma-Aldrich®. For each of the three experiments, the

tracer solution of RWT and  $\text{K}^{15}\text{NO}_3$  was injected at a constant rate of  $20 \text{ ml min}^{-1}$  for 24 h with a target  $\delta^{15}\text{N}$  value of  $+2000\text{‰}$  or greater. For each experiment, the injection solution was introduced to the stream upstream of a turbulence structure to ensure complete mixing of the solution and stream water. Each  $^{15}\text{NO}_3^-$  addition experiment commenced at 14:00 on 'Day 1' of the test. For each experiment, 10 in-stream points positioned longitudinally along the study reach (Figure 1) were sampled three times: twice during the injection and once 24 h after the injection was terminated. Sampling during the injection was completed at 2:00 and at 13:00 on 'Day 2'. Post-injection sampling was done at 13:00 on 'Day 3'. All samples were field filtered with a pre-combusted Whatman® GF/C 1.20  $\mu\text{m}$  filter, transferred into 250 ml high-density polyethylene (HDPE) bottles and frozen. These frozen samples were subsequently shipped to the laboratories at SUNY-ESF and the University of Calgary for chemical and isotopic analyses, respectively.

Table I. Characteristics of individual study reaches along Red Canyon Creek and date of experimental injection with  $^{15}\text{N}$ . Locations of the reaches are shown in Figure 1

	Reach A	Reach B	Reach C
Date of Injection experiment	24 June 2007	26 June 2007	28 June 2007
Metabolism dates	23 June to 25 June 2007	26 June to 28 June 2007	29 June to 1 July 2007
Reach length (m)	677	734 <sup>a</sup>	744
Average daytime discharge on day of injection ( $1 \text{ s}^{-1}$ )	182	200	59
Average night-time discharge on day of injection ( $1 \text{ s}^{-1}$ )	158	154	54
Major stream water ions	$\text{Ca}^{2+}$ , $\text{SO}_4^{2-}$ and $\text{HCO}_3^-$	$\text{Ca}^{2+}$ , $\text{SO}_4^{2-}$ and $\text{HCO}_3^-$	$\text{Ca}^{2+}$ and $\text{SO}_4^{2-}$
Average background nitrate concentration at time of experiment ( $\mu\text{mol}_c \text{ l}^{-1}$ )	0.71	1.30	0.17
$k_{\text{O}_2}$ ( $\text{day}^{-1}$ )	49	46	74
Water velocity ( $\text{m s}^{-1}$ )	0.17	0.15	0.22
Measured incoming shortwave radiation ( $\text{MJ m}^{-2} \text{ s}^{-1}$ ) <sup>b</sup>	33 (25 June 2007)	16 (27 June 2007)	32 (29 June 2007)
Stream temperature range ( $^{\circ}\text{C}$ ) <sup>c</sup>	11.4–23.7	10.5–21.4	14.7–23.7
Number of debris/log dams	1	4	0
Number of beaver dams	1	2	0

<sup>a</sup> Metabolism was measured over the first 593 m of this reach.

<sup>b</sup> Values are reported for the day on which mid-injection daytime sampling was done.

<sup>c</sup> Temperature ranges are for the dates on which metabolism measurements were made.

### Analytical techniques

Samples collected from each study reach were analysed at the Isotope Science Laboratory (ISL) at the University of Calgary (Alberta, Canada) for isotopic compositions. Stable isotopes of nitrogen were analysed using the denitrifier method (Sigman *et al.*, 2001). Denitrifying bacteria are injected into each aqueous sample and all nitrates present were converted to nitrous oxide ( $\text{N}_2\text{O}$ ) gas. A trace gas pre-concentrator was coupled with a Thermo-Finnigan Delta Plus XL isotope ratio mass spectrometer in continuous flow mode (CF-IRMS) to measure stable nitrogen isotope ratios using  $\text{N}_2\text{O}$ . Nitrogen isotope ratios are reported in the usual 'delta' notation as  $\delta^{15}\text{N}$  values in per mil (‰) with respect to atmospheric  $\text{N}_2$ . Four international reference materials were used to ensure precise and accurate results: United States Geological Survey (USGS) 32 (+180‰  $\pm$ 1.0), USGS 34 (−1.8‰  $\pm$ 0.2), USGS 35 (+2.7‰  $\pm$ 0.2) and International Atomic Energy Agency (IAEA)  $\text{NO}_3$  (+4.7‰  $\pm$ 0.2). The values in parentheses are the accepted IAEA values for  $\delta^{15}\text{N} \pm$  standard deviation. In addition, an internal laboratory standard (ISL- $\text{NO}_3$ ) with a known  $\delta^{15}\text{N}$  value was also analysed repeatedly yielding a  $\delta^{15}\text{N}$  value of +4.24‰  $\pm$ 0.27 ( $n=34$ ). Results were normalized using IAEA  $\text{NO}_3$  and USGS 34, while ISL- $\text{NO}_3$  and other reference materials were analysed daily as unknowns for QA/QC purposes. Precision and accuracy for analyses for natural abundance  $\delta^{15}\text{N}$  measurements are  $\pm$ 0.2‰ ( $2\sigma$  standard deviation).

In addition to nitrogen stable isotope data, the chemical composition of the obtained water samples was determined at SUNY-ESF including major anions ( $\text{NO}_3^-$ ,  $\text{SO}_4^{2-}$  and  $\text{Cl}^-$ ) and cations ( $\text{NH}_4^+$ ,  $\text{Na}^+$ ,  $\text{Ca}^{2+}$ ,  $\text{Mg}^{2+}$  and  $\text{K}^+$ ). Anion concentrations in each sample were determined by ion chromatography using a Dionex ICS 2000. Mean percent errors for anion analyses were 9, 5 and 7% for chloride, nitrate and sulfate, respectively. The minimum detection limit for nitrate was estimated as  $0.1 \mu\text{mol}_c \text{ l}^{-1}$ , which is the concentration equivalent of three times the standard deviation of replicate instrumental measurements of nitrate for an internal standard. Cation concentrations in each sample were measured using a Perkin-Elmer OPTIMA 3300DV inductively coupled plasma—optical emission spectrometer. Ammonium concentrations in each sample were measured using a Bran + Luebbe AutoAnalyzer.  $\text{HCO}_3^-$  concentrations were computed as the difference between the measured anion and cation concentrations.

### Calculating Net Aqueous Nitrate Uptake Length

'Net' nitrate uptake length and 'gross' uptake length were calculated using the background aqueous nitrate concentrations and the isotopic addition test results, respectively. The net nitrate uptake length was determined using ambient stream nitrate concentrations for Reaches A and B.

Both net and gross nitrate uptake lengths can be described as first-order decay functions based on the

decline in stream nitrate concentration per unit time (Stream Solute Workshop, 1990). We evaluated gross nitrate uptake lengths ( $S_w$ ) in the nitrate addition experiments because the short duration of the experiments only allows for consideration of gross uptake of nitrate and does not allow for re-mineralization or consideration of net nitrate loss (Payn *et al.*, 2005). In contrast, background nitrate concentrations downstream from a point source reflect the balance of both uptake of nitrate and remineralization of nitrogen and nitrification in the stream system and hence may capture the net uptake of nitrate ( $S_{w,net}$ ), rather than simply the gross uptake ( $S_w$ ). We designated uptake lengths determined from background nitrate chemistry as 'net nitrate uptake lengths' and uptake rates from  $^{15}\text{N}$  tracer injection experiments as 'gross nitrate uptake lengths'.

We assumed nitrate uptake followed first-order decay, which can be expressed as:

$$\ln C_t = \ln C_o - k_c t \quad (1)$$

where  $C_t$  was the nitrate concentration at time  $t$  after introduction to the stream system ( $\mu\text{mol}_c \text{ l}^{-1}$ ),  $C_o$  was the initial nitrate concentration ( $\mu\text{mol}_c \text{ l}^{-1}$ ) and  $k_c$  was the nitrate uptake rate coefficient ( $\text{min}^{-1}$ ) (Newbold *et al.*, 1981). Using the link between distance and time (i.e. stream velocity), this first-order decay function can be transformed into a loss per distance travelled downstream:

$$\ln C_x = \ln C_o - (1/S_{w,net})x \quad (2)$$

where  $C_x$  was the nitrate concentration at distance  $x$  downstream of where nitrate was introduced to the stream ( $\mu\text{mol}_c \text{ l}^{-1}$ ),  $C_o$  was the nitrate concentration at a distance of zero (i.e. the location of a natural point source,  $\mu\text{mol}_c \text{ l}^{-1}$ ),  $1/S_{w,net}$  was the inverse of the uptake length ( $\text{m}^{-1}$ ) and  $x$  was the distance downstream of the source site (m). The  $1/S_{w,net}$  term was equal to  $k_c/\text{velocity}$  (Newbold *et al.*, 1981).

The net nitrate uptake length ( $S_{w,net}$ ) can be determined from the steady-state decline in the background nitrate concentration with distance from a naturally occurring point source, under ambient conditions. To calculate a background nitrate spiralling length, the natural logarithm of the ambient nitrate concentration was plotted versus distance in the stream. The nitrate spiralling length was then calculated as the negative inverse of the slope of the best-fit regression through the data. The net linear nitrate uptake rate ( $U_{net}$ , in  $\mu\text{mol}_c \text{ s}^{-1} \text{ m}^{-2}$ ) was then calculated as:

$$U_{net} = \frac{(C_{\text{mean}} \times Q)}{(S_{w,net} \times w)} \quad (3)$$

where  $C_{\text{mean}}$  is the mean background nitrate concentration along the respective reach ( $\mu\text{mol}_c \text{ l}^{-1}$ ),  $Q$  is the stream-flow rate ( $\text{l s}^{-1}$ ) and  $w$  is the stream width (m).

#### Calculating gross nitrate uptake length from isotopic additions

Gross nitrate uptake lengths (in contrast to net nitrate uptake lengths) for the individual experimental reaches

were determined using the results of the respective isotopic addition experiments and methods presented in Mulholland *et al.* (2008), which are briefly summarized here. Downstream changes in  $\delta^{15}\text{N}$  and nitrate concentrations were monitored at 10 stream water sampling locations in each study reach, as described above. To compute nitrate uptake length,  $\delta^{15}\text{N}$  values were converted into tracer  $^{15}\text{N}$  fluxes. The  $\ln(\text{tracer } ^{15}\text{N} \text{ flux})$  was used in the regression over distance to determine the nitrate loss from the stream. First,  $\delta^{15}\text{N}$  values were converted to  $^{15}\text{N}/(^{15}\text{N}+^{14}\text{N})$  ratios, the isotopic mole fraction (MF) of  $^{15}\text{N}$ , by the following equation:

$$\text{MF} = \frac{^{15}\text{N}}{^{15}\text{N}+^{14}\text{N}} = \frac{\left(\frac{\delta^{15}\text{N}}{1000} + 1\right) \times 0.0036765}{1 + \left(\left(\frac{\delta^{15}\text{N}}{1000} + 1\right) \times 0.0036765\right)} \quad (4)$$

where 0.0036765 represents the  $^{15}\text{N}:^{14}\text{N}$  ratio of atmospheric  $\text{N}_2$  with a  $\delta^{15}\text{N}$  value of 0‰. The tracer  $^{15}\text{NO}_3^-$  mass flux at each sampling station,  $^{15}\text{N}_{\text{flux},i}$  ( $\mu\text{g s}^{-1}$ ), was calculated by the following equation:

$$^{15}\text{N}_{\text{flux},i} = (\text{MF}_i \times [\text{NO}_3 - \text{N}]_i \times Q_i)_{\text{injection}} - (\text{MF}_i \times [\text{NO}_3 - \text{N}]_i \times Q_i)_{\text{pre-injection}} \quad (5)$$

where  $\text{MF}_i$  is the isotopic mole fraction of  $^{15}\text{N}$  at sampling station  $i$ ,  $[\text{NO}_3 - \text{N}]_i$  was the stream water nitrate concentration as nitrogen at sampling station  $i$  ( $\mu\text{g l}^{-1}$ ) and  $Q_i$  is the stream discharge at sampling station  $i$  ( $\text{l s}^{-1}$ ). Pre-injection  $^{15}\text{NO}_3^-$  mass flux was subtracted from the  $^{15}\text{NO}_3^-$  mass flux measured during the injection experiment to isolate the tracer  $^{15}\text{NO}_3^-$  flux from the additional background flux of  $^{15}\text{NO}_3^-$ . Stream discharge at each sampling station ( $Q_i$ ) was calculated based on the dilution of the conservative tracer (RWT) by:

$$Q_i = \frac{Q_{\text{inj}} \times C_{\text{inj}}}{C_{\text{p},i}} \quad (6)$$

where  $Q_{\text{inj}}$  is the pump rate of the injection solution ( $\text{l s}^{-1}$ ),  $C_{\text{inj}}$  was the concentration of RWT in the injection solution ( $\mu\text{g l}^{-1}$ ) and  $C_{\text{p},i}$  was the concentration of RWT in the stream water at the plateau of the injection at station  $i$  ( $\mu\text{g l}^{-1}$ ).

The gross nitrate uptake rate coefficient was calculated as the slope of  $\ln(^{15}\text{N}_{\text{flux},i})$  as a function of distance from the injection point for the sampling sites within each of the study reaches. The nitrate uptake length ( $S_w$ , m) of each reach was calculated as the inverse of that slope. The gross linear nitrate uptake rate ( $U_{\text{net}}$ , in  $\mu\text{mol}_c \text{ s}^{-1} \text{ m}^{-2}$ ) was then calculated as:

$$U_{\text{gross}} = \frac{(C_{\text{mean}} \times Q)}{(S_w \times w)} \quad (7)$$

where  $C_{\text{mean}}$  is the mean background nitrate concentration along the respective reach ( $\mu\text{mol}_c \text{ l}^{-1}$ ),  $Q$  is the reach-average streamflow rate ( $\text{l s}^{-1}$ ) and  $w$  is the average stream width (m).

### Air–water gas exchange

We calculated the piston velocity and air–water gas exchange of  $O_2$  for each reach using additions of sulphur hexafluoride ( $SF_6$ ), a tracer that evades at a rate proportional to  $O_2$  evasion rates (Wanninkhof *et al.*, 1990; Cole and Caraco, 1998). We collected triplicate dissolved gas samples at five stations downstream from each release site and measured the decline in  $SF_6$  concentrations using a gas chromatograph with an electron capture detector (Shimadzu Gas Chromatograph 14A). Values for  $k_{SF_6}$  ( $m^{-1}$ ) were measured from the decline in  $SF_6$  downstream and used to calculate reach piston velocity ( $k_{SF_6}$ ;  $m\ min^{-1}$ ) and reaeration coefficient ( $day^{-1}$ ). Using the ratios of gas transfer velocities and temperature-adjusted Schmidt numbers for  $SF_6$  and  $O_2$ , a reach-specific  $k_{O_2}$  was calculated from  $k_{SF_6}$  (Wanninkhof, 1992; Cole and Caraco, 1998).

### Ecosystem metabolism

We measured gross primary production (GPP) and ecosystem respiration (ER) for each of the three stream reaches using the two-station, open-channel, dissolved oxygen ( $dO_2$ ) method (Odum, 1956). We placed one Hydrolab MiniSonde (Hach Environmental) at either end of each  $^{15}N$  tracer reach during 23–25 June, 26–28 June and 29 June–1 July 2007 (A1–A10, B1–B9 and C1–C10, respectively). The MiniSondes measured changes in  $dO_2$  concentrations every 10 min for 2-day cycles during or within 1 day of the  $^{15}N$  tracer releases for each reach. We calculated GPP and ER based on the changes in  $dO_2$  along each reach (Hall *et al.*, 2007):

$$\begin{aligned} \text{Instant metabolism (g } O_2 \text{ m}^{-2} \text{ min}^{-1}) \\ = z \left[ \frac{(C_t - C_0)}{t} \right] - k_{O_2} (O_{2\text{sat}} - O_2) \end{aligned} \quad (8)$$

where  $C_t$  and  $C_0$  are the dissolved oxygen concentrations at downstream and upstream sites ( $g\ O_2\ m^{-3}$ ),  $t$  is water travel time between upstream and downstream sites (min),  $k_{O_2}$  is the piston velocity for  $O_2$  ( $m\ min^{-1}$ ),  $O_{2\text{sat}} - O_2$  is the difference between in-stream  $dO_2$  and saturation ( $g\ O_2\ m^{-3}$ ) and  $z$  is stream depth (m).

ER was measured at night when only reaeration and ER were contributing to instant metabolism calculations. After accounting for ER, GPP was calculated as the area under each 24-h  $dO_2$  curve (Odum, 1956; Hall *et al.*, 2007). We did not correct metabolism estimates for groundwater discharge along any of the three  $^{15}N$  tracer addition reaches because we did not observe significant changes in streamflow or dilution of RWT, a conservative tracer, along the individual experimental reaches. We did adjust day and night ER calculations based on higher discharge during the day versus night (Table I).

## RESULTS

### Spatial and temporal patterns of background stream water chemistry

Background stream water nitrate concentrations in Red Canyon Creek were low at the time of the experiments, with all observed concentrations  $<2.5\ \mu\text{mol}_c\ l^{-1}$  (Figure 2). Major ion chemistry in Red Canyon Creek is dominated by calcium, magnesium, sulfate and bicarbonate, which combined, made up 98% of the total dissolved solids, in  $\mu\text{mol}_c\ l^{-1}$ .

Stream solute data for day and night were plotted (Figure 2) as the solute concentration versus distance from the most upstream point of all experimental reaches (i.e. the Reach C injection site). Daytime concentrations are for the pre-injection (i.e. Day 1, 13:00), daytime mid-injection (i.e. Day 2, 13:00) and post-injection (Day 3, 13:00) samples. Night-time concentration values are for the night-time mid-injection sample (Day 2, 2:00), which was the only sampling done at night.

Three distinct groups of nitrate concentration values were observed (Figure 2) over the entire Red Canyon Creek experimental reach (i.e. C1–A10, Figure 1). The first group of nitrate concentrations was observed along Reach C (C1–C10), which is just upstream of the confluence of Red Canyon Creek with its major tributaries, Cherry Creek and Barrett Creek. Along this segment, nitrate concentrations during the daytime were very low ( $<0.2\ \mu\text{mol}_c\ l^{-1}$ ) with very little change between upstream and downstream sites (less than 4% change each day). Sample station C1 on Day 2 did not show any detectable nitrate. Concentrations of nitrate at night showed a 17% increase from  $0.28\ \mu\text{mol}_c\ l^{-1}$  upstream to  $0.34\ \mu\text{mol}_c\ l^{-1}$  downstream, but these small changes may have been due to natural and analytical variation because these values were near the detection limit for chemical analyses. Nitrate concentrations at night were higher than during the day at every sampling site.

The second group of concentrations was observed along the upstream portion of Reach B (B1–B4), just downstream of the confluence of Red Canyon Creek with Cherry Creek and Barrett Creek. Pre-injection sampling showed that tributaries had higher nitrate concentrations than the main stem of Red Canyon Creek, causing a rise in nitrate in Red Canyon Creek between sampling sites C10 and B1. From B1 to B4, nitrate concentrations averaged  $0.83$  and  $0.87\ \mu\text{mol}_c\ l^{-1}$  during the day and night, respectively. During the day, nitrate concentrations consistently declined with distance, but only by 3–9%. At night, nitrate concentrations varied by only 4%. There were no significant differences ( $p > 0.05$ ) between the average daytime and night-time nitrate concentrations from B1 through B4.

The third group of nitrate concentrations is marked by a greater than twofold increase in nitrate between B4 and B5 and then a general decrease with distance from sites B5 to A10 during the daytime and at night (Figure 2). We observed an average daytime nitrate concentration

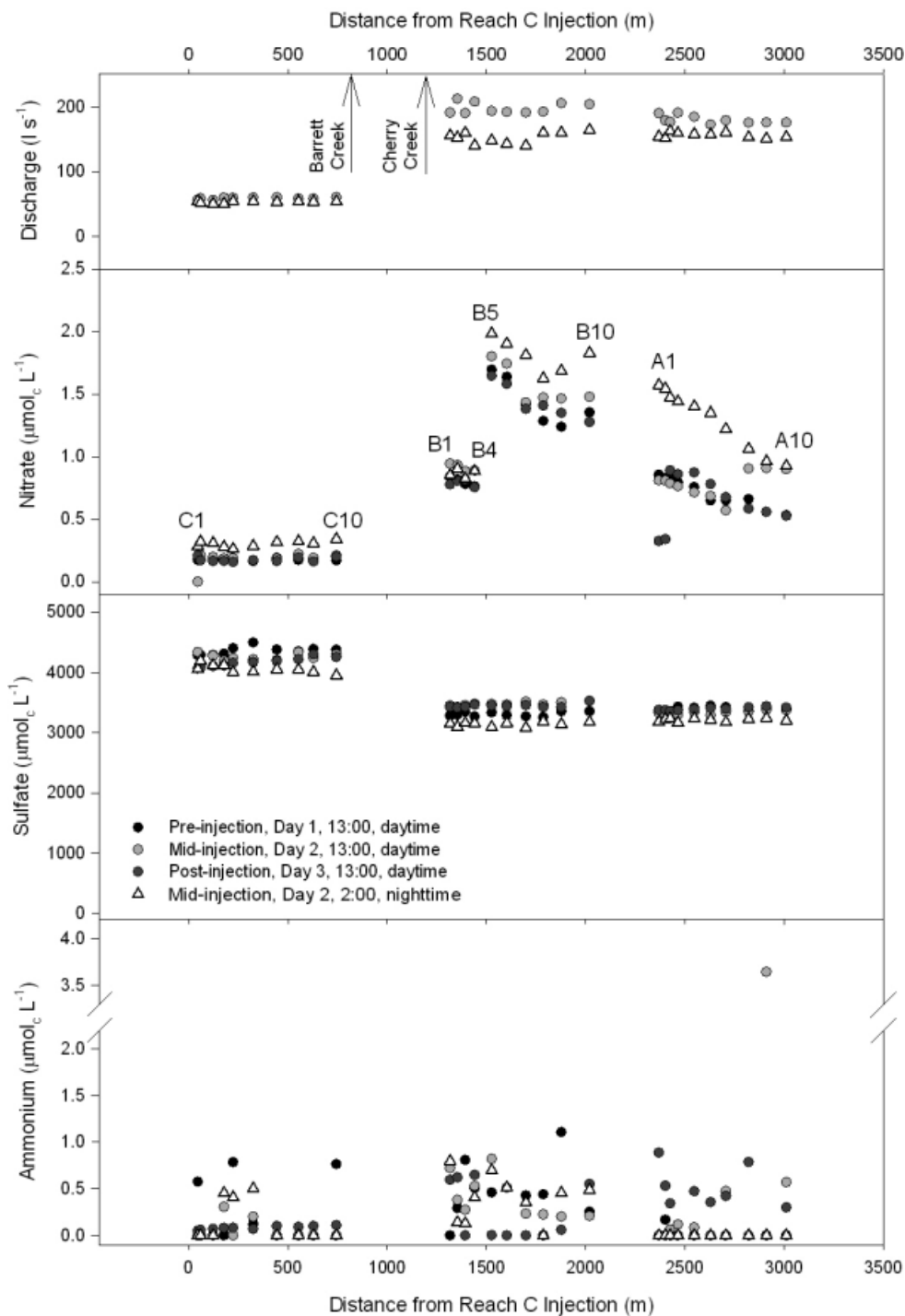


Figure 2. Observed stream discharge, nitrate, sulfate and ammonium concentrations in stream water along the experimental reaches

decrease of 62% from 1.7  $\mu\text{mol}_c \text{ l}^{-1}$  upstream (B5) to 0.7  $\mu\text{mol}_c \text{ l}^{-1}$  downstream (A10). Given the consistency of the Day 1 and Day 2 13:00 nitrate concentration measurements at other sites and at other reaches, the causes of small increases in the three most downstream samples on Day 2 are not known. Night-time nitrate concentrations were greater than daytime concentrations from B5 to A10 (mean of 1.5  $\mu\text{mol}_c \text{ l}^{-1}$  vs 1.0  $\mu\text{mol}_c \text{ l}^{-1}$ , respectively). Night-time nitrate concentrations showed a steady 53% decline from 2.0  $\mu\text{mol}_c \text{ l}^{-1}$  upstream to 0.9  $\mu\text{mol}_c \text{ l}^{-1}$  downstream (Figure 2).

In sharp contrast to the nitrate concentrations, sulfate, chloride, sodium, magnesium and potassium concentrations did not show any marked changes in concentration (i.e. <5% increase or decrease) from upstream to downstream at night or during the day, except for the notable change in solute concentrations at the confluence of Barrett Creek and Cherry Creek tributaries. Sulfate concentrations are shown as an example of the trends also present for the other ions listed above (Figure 2). These results suggest that these other ions were not markedly affected by groundwater contributions along the stream,

which is consistent with measurements of streamflow by dilution gauging during tracer injections (Figure 2) and other studies that have shown little groundwater contribution at Red Canyon Creek (Lautz and Siegel, 2006; Lautz *et al.*, 2006). Ammonium concentrations were generally low in stream water ( $<2.0 \mu\text{mol}_c \text{ l}^{-1}$ ) with no discernable pattern with distance downstream (Figure 2).

*Net nitrate uptake*

Using background aqueous nitrate concentrations in Red Canyon Creek, we calculated daytime and night-time net nitrate uptake lengths ( $S_{w,\text{net}}$ ). Nitrate uptake for Reach B was calculated starting at site B5, a nitrate point source. Nitrate concentrations did not need to be corrected for dilution because there was no detectable change in streamflow due to groundwater discharge along the reach (Figure 2). Daytime and night-time  $S_{w,\text{net}}$  were calculated to be 1300 and 1170 m, respectively, for Reach A. Daytime and night-time  $S_{w,\text{net}}$  were calculated to be 2020 and 4330 m, respectively, for Reach B (Figure 3, Table II).

We are confident that a point source of nitrate exists between B4 and B5 because we consistently measured a sudden increase in nitrate between these two points at night and during the day. The increase in nitrate concentration was not concurrent with an increase in any other major ion or an increase in streamflow that would suggest influx of a point source of nitrate-rich water between B4 and B5 (Figure 2). We also see a predictable decline in nitrate with distance downstream of this location (B5 to A10). Unfortunately, analysis for nitrate was done after returning from the field site and the nature of the point source could not be confirmed visually. No other large changes in ion concentrations (chloride, sulfate, calcium, magnesium or sodium) occurred at this location, so it is likely an organic source of N.

*Stream water  $\delta^{15}\text{N}_{\text{nitrate}}$*

Prior to the  $^{15}\text{NO}_3^-$  additions,  $\delta^{15}\text{N}$  values averaged for each reach were +6, +7 and +5‰ for Reaches A, B

Table II. Nitrate uptake and spiralling lengths from injection experiments and background nitrate chemistry as well as rates of ecosystem metabolism for Reaches A, B and C

	Reach A	Reach B	Reach C
<i>Net uptake lengths from background nitrate chemistry</i>			
$S_{w,\text{net}}$ , daytime (m)	1300	2020	—
$S_{w,\text{net}}$ , night-time (m)	1170	4330	—
<i>Gross uptake lengths from injection experiments</i>			
$S_w$ , daytime (m)	502	650	657
$S_w$ , night-time (m)	1020	3140	1960
<i>Ecosystem metabolism rates</i>			
GPP, gross primary production (g $\text{O}_2 \text{ m}^{-2} \text{ day}^{-1}$ )	6.3	4.5	1.2
ER, ecosystem respiration (g $\text{O}_2 \text{ m}^{-2} \text{ day}^{-1}$ )	-12.8	-5.8	-2.5
NEP, net ecosystem production (GPP+ER; g $\text{O}_2 \text{ m}^{-2} \text{ day}^{-1}$ )	-6.5	-1.3	-1.3
<i>Nitrate regeneration parameters</i>			
$C_{\text{mean}}$ , daytime ( $\mu\text{mol l}^{-1}$ )	0.79	1.30	—
$C_{\text{mean}}$ , night-time ( $\mu\text{mol l}^{-1}$ )	1.18	1.43	—
$U_{\text{net}}$ , daytime ( $\mu\text{mol s}^{-1} \text{ m}^{-2}$ )	0.035	0.038	—
$U_{\text{net}}$ , night-time ( $\mu\text{mol s}^{-1} \text{ m}^{-2}$ )	0.056	0.016	—
$U_{\text{gross}}$ , daytime ( $\mu\text{mol s}^{-1} \text{ m}^{-2}$ )	0.092	0.117	—
$U_{\text{gross}}$ , night-time ( $\mu\text{mol s}^{-1} \text{ m}^{-2}$ )	0.065	0.023	—
Nitrate regeneration rate, daytime ( $\mu\text{mol s}^{-1} \text{ m}^{-2}$ )	0.056	0.080	—
Nitrate regeneration rate, night-time ( $\mu\text{mol s}^{-1} \text{ m}^{-2}$ )	0.0083	0.0062	—

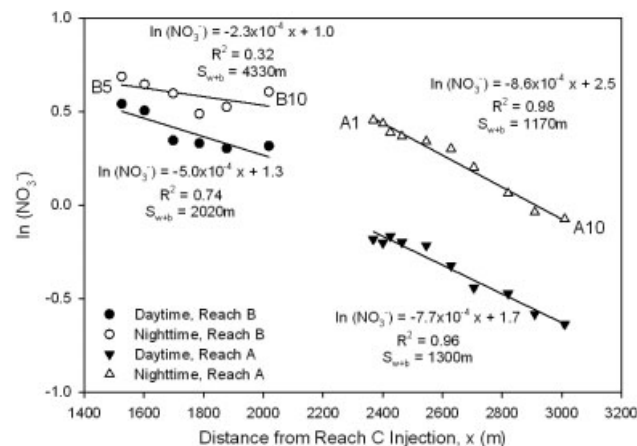


Figure 3. Natural log of observed nitrate concentrations with distance from B5 to A10. Linear regression was used to generate the lines shown and associated equations,  $R^2$  values and  $S_{w,\text{net}}$  values

and C, respectively ( $n = 10$ ). One day after the end of the tracer injections, the  $\delta^{15}\text{N}$  values had generally returned to values close to background except for Reach C (+8, +8 and +24‰ for Reaches A, B and C, respectively) (Figure 4).

Along Reach A,  $\delta^{15}\text{N}$  values decreased from upstream to downstream during the injection during both day and night, but  $\delta^{15}\text{N}$  values decreased more markedly from upstream to downstream during the day (Figure 4).  $\delta^{15}\text{N}$  values were greater during the daytime than the night-time during the injection at all sites, excluding A8, A9 and A10.

Similar to Reach A,  $\delta^{15}\text{N}$  values decreased with distance at night during the injection along Reach B. However, there was a slight increase in  $\delta^{15}\text{N}$  from B1 to B4, and a marked decrease from B4 to B5 and a more gradual decrease from B5 to B10. The change in isotopic composition between B4 and B5 corresponds

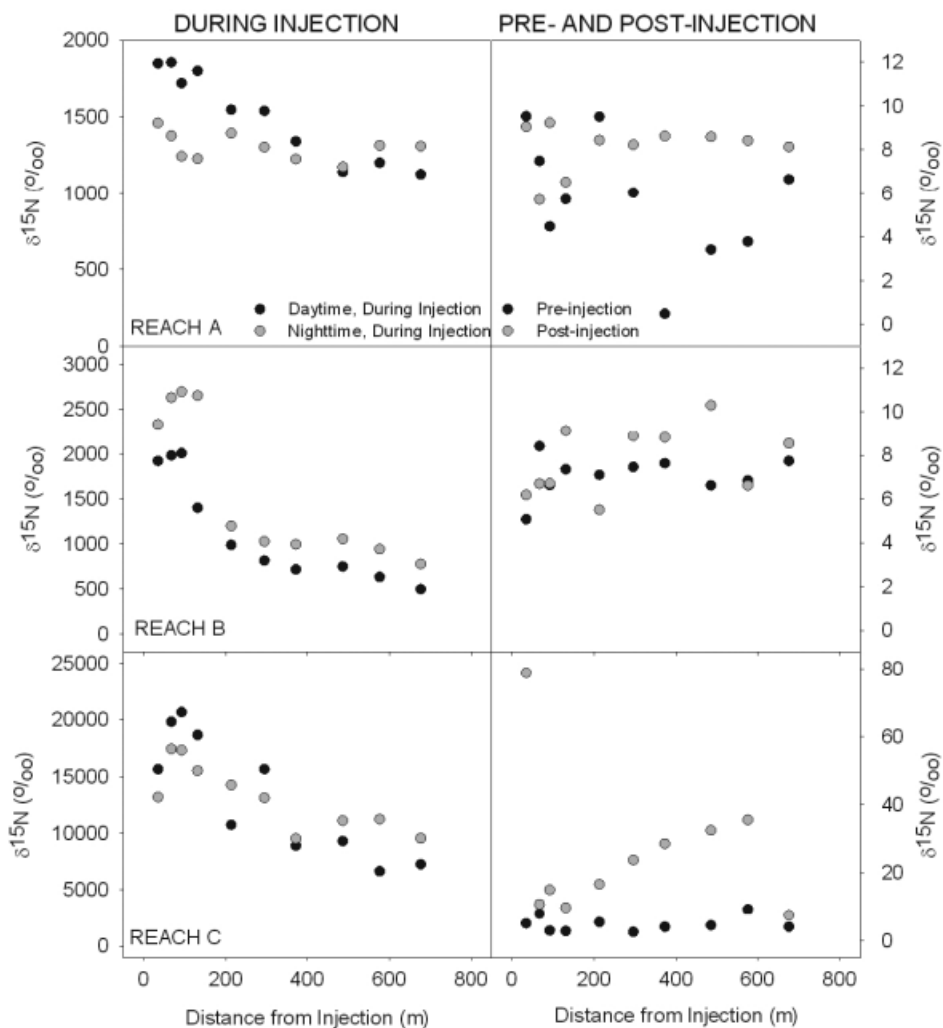


Figure 4.  $\delta^{15}\text{N}_{\text{nitrate}}$  values with distance along each reach before, during and after the injection experiments

with the change in background nitrate concentrations (Figure 2). During daytime,  $\delta^{15}\text{N}$  values also decreased with distance.  $\delta^{15}\text{N}$  values increased slightly from B1 to B3 and decreased from B4 to B10 (Figure 4). The  $\delta^{15}\text{N}$  values were always greater during the night than the day.

As observed in Reaches A and B,  $\delta^{15}\text{N}$  values decreased with distance during the experimental injection at night and during the day along Reach C. Overall,  $\delta^{15}\text{N}$  values were much higher during the Reach C experiment (up to 17 400‰), relative to the other two experiments where the maximum  $\delta^{15}\text{N}$  value was 2690‰, explaining why post-injection  $\delta^{15}\text{N}$  values did not completely return to pre-injection levels (Figure 4).

#### Isotopic nitrate uptake length

Similar to the net nitrate uptake length ( $S_{w,\text{net}}$ ) calculation, nitrogen isotopes were used to calculate daytime and night-time gross uptake lengths ( $S_w$ ) for each individual study reach. The regression of  $^{15}\text{N}$  flux with distance was used to calculate  $S_w$ , as described in the methods (Figure 5).

Anomalous data was omitted from these analyses in order to facilitate calculation of  $S_w$  using  $^{15}\text{N}$  flux.

Reach A exhibited an unexpected increase in nitrate concentration between A7 and A8 during one of the sampling events (Day 2, 13:00) that did not follow the pattern exhibited during the other daytime sampling events. The observed increase could not be attributed to any known source of nitrate to the stream or any tributary to Red Canyon Creek and a similar increase was not observed during the Day 1, 13:00, or Day 3, 13:00, sampling. Hence, we used data from A1 to A7 to calculate daytime  $S_w$  for Reach A. The complete data set (A1 to A10) was used to calculate night-time  $S_w$  for Reach A.

$S_w$  was 502–657 m during the day and 1020–3140 m at night for Reaches A, B and C, respectively (Table II, Figure 5).  $S_w$  was shortest along Reach A, both during the day and night. Night-time  $S_w$  values were between 2.0 and 4.8 times the daytime values of  $S_w$ .

#### Hyporheic zone pore water chemistry

For our study the hyporheic zone pore water chemistry was generally similar to that of stream water with concentrations of calcium, magnesium, sulfate and bicarbonate comprising 96% of the total dissolved solids in the hyporheic zone, in  $\mu\text{mol l}^{-1}$ . Concentrations of sulfate

were significantly lower in the hyporheic zones upstream of the dams ( $p < 0.01$ ), relative to the corresponding downstream hyporheic zones and the stream water (Figure 6). Concentrations of nitrate in the hyporheic zone were generally lower than in stream water at upstream locations around the man-made dam and the beaver dam (Figure 6). The hyporheic zone downstream of the man-made dam showed substantial increases in nitrate concentrations above stream water (Figure 6). The downstream hyporheic zone at the beaver dam showed a slight increase in nitrate concentration at DB-3. Nitrate concentrations from upstream to downstream differed at the man-made dam ( $p < 0.01$ ), but not at the beaver dam ( $p = 0.26$ ).

Overall, ammonium concentrations in the hyporheic zone were greater than in stream water (Figure 7). Generally, ammonium concentrations were greatest in the upstream hyporheic zones (Figure 7). Concentrations of ammonium and nitrate were generally inversely correlated in the hyporheic zone (Figure 7). Ammonium concentrations were significantly higher upstream versus downstream at the man-made dam ( $p < 0.01$ ) and at the beaver dam ( $p = 0.01$ ).

#### Hyporheic zone $\delta^{15}N_{\text{nitrate}}$

In the hyporheic zone around the beaver dam,  $\delta^{15}N$  values continuously increased from Day 1 ( $-2$  to  $+4\%$ ) to Day 3 ( $+7$  to  $+14\%$ ) of the experimental injections (Figure 8), but the increase was generally less than  $15\%$ . In the hyporheic zone around the man-made dam, the upstream and downstream segments of the hyporheic zone responded differently during the  $^{15}N$  additions. On Day 1,  $\delta^{15}N$  values of nitrate were similar upstream and downstream of the dam, ranging from  $+5.1$  to  $+11.8\%$  upstream and from  $+7.2$  to  $+9.3\%$  downstream. Downstream hyporheic zone nitrate samples became much more  $^{15}N$  enriched on Day 2, with  $\delta^{15}N$  values ranging from  $51$  to  $392\%$ , but returned to pre-injection levels on Day 3 (Figure 8). Upstream hyporheic zone samples showed only small increases in  $\delta^{15}N$  values similar to those observed at the beaver dam.

#### Air–water gas exchange and ecosystem metabolism

Reaeration coefficients ( $k_{O_2}$ ;  $\text{day}^{-1}$ ) were 49, 46 and 74 for Reaches A, B and C, respectively (Table I). All three reaches of Red Canyon Creek had strong diel cycles in rates of instant metabolism (Figure 9). Over two full 24-h measurement cycles, the average rates of GPP in Reaches A, B and C were  $6.3$ ,  $4.5$  and  $1.3$   $\text{g O}_2 \text{ m}^{-2} \text{ day}^{-1}$ ; average rates of ER in A, B and C were  $-12.8$ ,  $-5.8$  and  $-2.5$   $\text{g O}_2 \text{ m}^{-2} \text{ day}^{-1}$ . All three reaches were net heterotrophic ( $\text{ER} > \text{GPP}$ ) over both 24-h cycle measurements (Table II).

## DISCUSSION

#### Nitrate uptake and spiralling

Chemical nitrate salt addition tracer studies often overestimate  $S_w$  due to relatively large increases in nitrate

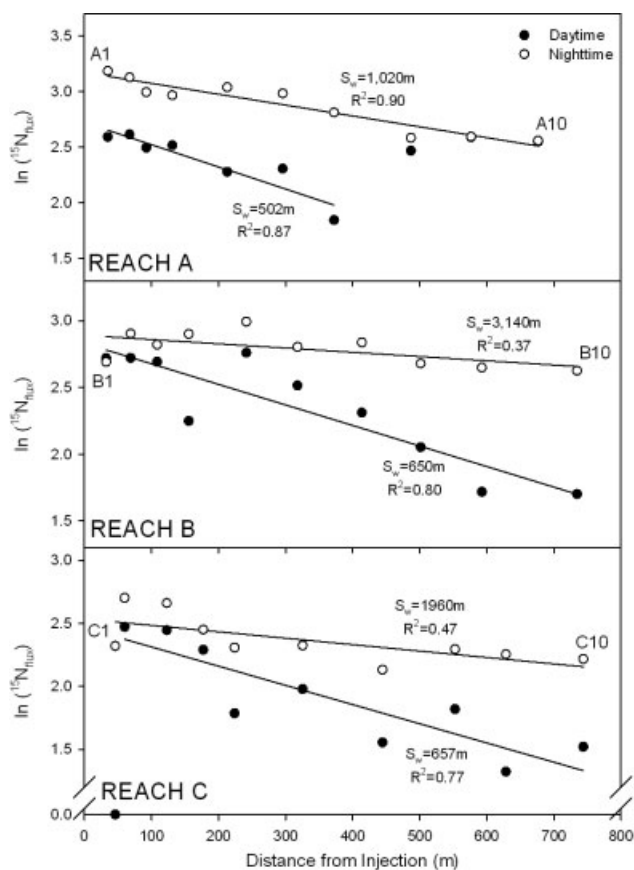


Figure 5. Natural log of the  $^{15}N_{\text{nitrate}}$  flux with distance for each experimental reach. Linear regression was used to generate the lines shown and the  $R^2$  values. The inverse slope of the regression lines is given as nitrate uptake length. Note that symbols for daytime A9 and A10 are not visible behind the nighttime symbols

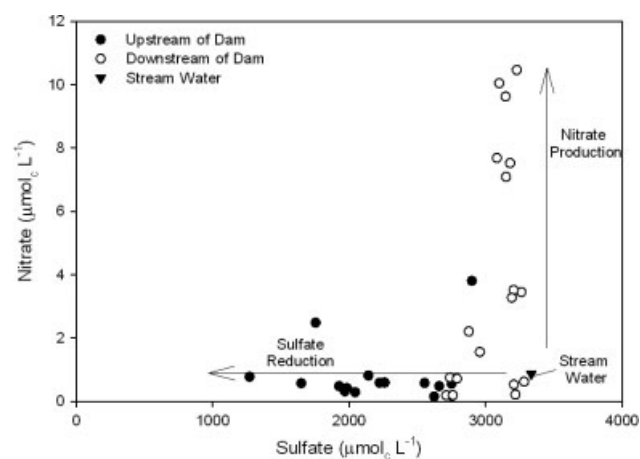


Figure 6. Nitrate versus sulfate concentrations in the stream and the hyporheic zone upstream and downstream of the man-made log dam and the beaver dam

concentrations in the stream (Mulholland *et al.*, 2002). Increases in nitrate concentrations greatly above ambient conditions may exceed the capacity of the stream system to transform and remove nitrate. In a previous study in Red Canyon Creek, Lautz and Siegel (2007) found that using a nitrate salt addition approach, two out of three study reaches in the Red Canyon Creek watershed did

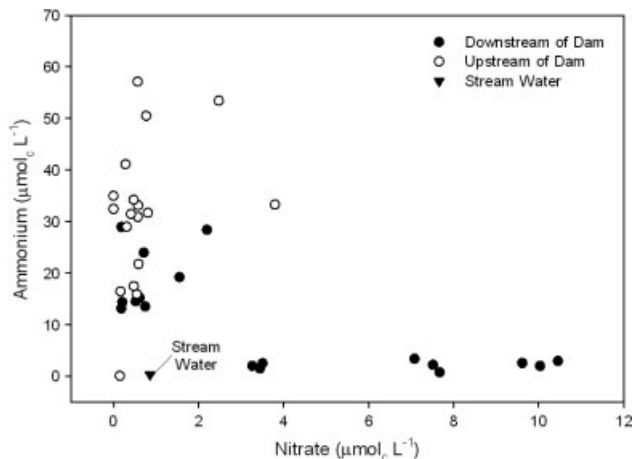


Figure 7. Ammonium versus nitrate concentrations in the stream and the hyporheic zone upstream and downstream of the man-made log dam and the beaver dam

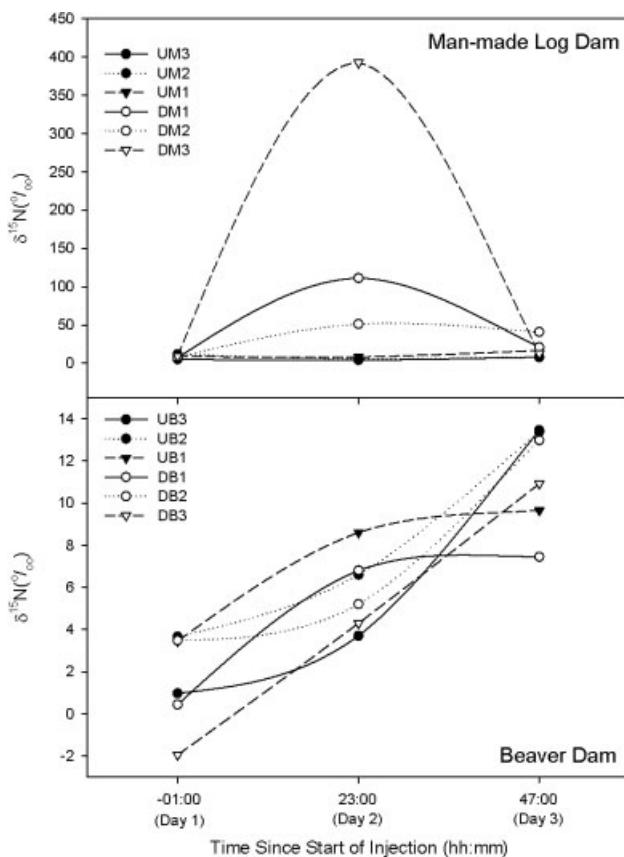


Figure 8.  $\delta^{15}\text{N}$  values in the hyporheic zone around the man-made log dam and the beaver dam before, during and after the isotopic tracer injection experiment

not show nitrate uptake. One of their study reaches that had undetectable  $S_w$  overlapped spatially with our Reach C, which had the longest  $S_w$  and the lowest ambient nitrate concentration in this study. The one reach that did not show nitrate uptake in the Lautz and Siegel (2007) study, Lower Red Canyon Creek, overlapped spatially with our Reach A and a similar daytime  $S_w$  was observed ( $S_w = 500$  m). All three reaches in this study, regardless of ambient nitrate concentration or stream discharge,

showed measurable  $S_w$  using the  $^{15}\text{N}$  tracer injection approach. This suggests that the nitrate salt addition approach used previously in Red Canyon Creek may have saturated uptake mechanisms in some reaches. Both the background chemical and  $^{15}\text{N}$  addition approaches utilized in this study did not increase the ambient stream water nitrate concentrations.

Daytime  $S_w$  (502, 650 and 657 m for Reaches A, B and C, respectively) and daytime  $S_{w,\text{net}}$  (1300 and 2020 m for Reaches A and B, respectively) were generally shorter than night-time  $S_w$  (1020, 3140 and 1960 m for Reaches A, B and C, respectively) and night-time  $S_{w,\text{net}}$  (1170 and 4330 m for Reaches A and B, respectively) (Table II). Night-time values were approximately two to five times the length of daytime values for the  $^{15}\text{N}$  injection  $S_w$  calculations as well as the  $S_{w,\text{net}}$  calculations, with the exception of the  $S_{w,\text{net}}$  values along Reach A. Diurnal fluctuations in nitrate uptake suggest that autotrophs play an important role in the consumption of nitrate at Red Canyon Creek (Mulholland *et al.*, 2006). Shorter daytime  $S_w$  and  $S_{w,\text{net}}$  values are likely a function of autotrophic activity and the concomitant utilization of nitrate by plants and algae (Hall and Tank, 2003; Fellows *et al.*, 2006; Mulholland *et al.*, 2006). Recent results from 72 different streams in the United States and Puerto Rico found a negative relationship between  $S_w$  and GPP; autotrophic  $\text{NO}_3^-$  uptake decreased  $\text{NO}_3^-$  uptake lengths (Hall *et al.*, 2009b). We found the same relationship between GPP and  $S_w$  in the three Red Canyon Creek reaches: Reach A had the shortest  $S_w$  and the highest GPP and Reach C had the longest  $S_w$  and the lowest GPP (Table II).

Solar radiation could impact uptake lengths through a decrease in autotrophic assimilation (Fellows *et al.*, 2006; Mulholland *et al.*, 2006). Total incoming solar radiation ranged from 29 to 33  $\text{MJ m}^{-2}$  between 24 June and 29 June, except for 27 June, which had only 16  $\text{MJ m}^{-2}$  of incoming solar radiation (Table I). Although GPP was lower on 27 June (Figure 9), it does not appear that lower solar radiation and GPP substantially increased  $S_w$ , perhaps due to a simultaneous increase in ER (Table II).

Regression lines for  $S_w$  and  $S_{w,\text{net}}$  using daytime observations had the best fit, with  $R^2$  values ranging from 0.74 to 0.96 (Figures 3 and 5). Night-time observations showed more scatter around the regression line, with  $R^2$  values ranging from 0.37 to 0.98 (Figures 3 and 5). Greater uptake during daytime hours caused the slope of the regression lines to be higher, due to more rapid removal of nitrate from the system. The stronger relationship and greater slope between nitrate concentration and distance during the daytime, compared to at night, indicate that primary production dominates the removal of N.

Net nitrate uptake lengths ( $S_{w,\text{net}}$ ) were generally longer than nitrate uptake lengths ( $S_w$ ). This is expected, provided that  $S_{w,\text{net}}$  includes the additional effects of mineralization and nitrification which return nitrate to the water, and suggests that our assumptions regarding the point source in Red Canyon Creek and the equilibrium

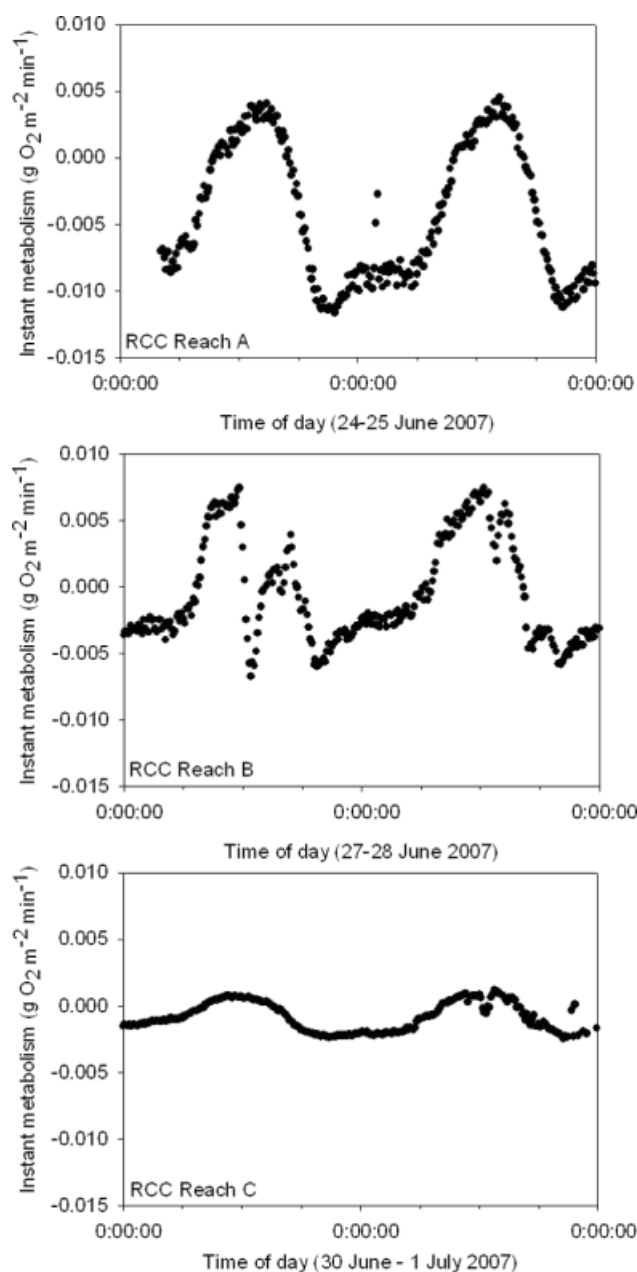


Figure 9. Diel instant metabolism over 48-h periods for all three reaches (A–C) of Red Canyon Creek, WY. All axes are on the same scale for between-reach comparisons

conditions downstream are accurate. Estimates of  $S_{w,net}$  using the background nitrate chemistry reflect an approximation of steady-state decline in the nitrate concentration with distance that is the net sum of nitrate uptake factors (i.e. denitrification and/or assimilatory nitrate reduction) and nitrate production factors (i.e. mineralization of organic matter forming ammonium followed by nitrification). In contrast,  $^{15}\text{N}$  methods reflect only the distance that a nitrate molecule remains in the stream in the dissolved phase before uptake. Given the limited time of the 24-h  $^{15}\text{N}$  injection, the system is not allowed to reach steady-state conditions and therefore does not include re-mineralization of organic matter (Payn *et al.*, 2005). By taking the difference between the net uptake rate ( $U_{w,net}$ ) and the gross uptake rate ( $U_w$ ), we can

approximate the nitrate regeneration rate in Red Canyon Creek. In Reaches A and B, the nitrate regeneration rate was approximately  $0.056\text{--}0.080\ \mu\text{mol s}^{-1}\ \text{m}^{-2}$  during the day and  $0.0062\text{--}0.0083\ \mu\text{mol s}^{-1}\ \text{m}^{-2}$  at night. An estimate of nitrate regeneration rates is unique to this study because we were able to compare nitrate loss during isotopic additions to background nitrate loss under equilibrium conditions. At other locations, where point sources of nitrate are present, similar nitrate regeneration rates could also be derived.

#### *Patterns in hyporheic zone pore water chemistry data*

Although diurnal fluctuations in  $S_w$  and  $S_{w,net}$  suggest that autotrophs in the water column may be primarily responsible for nitrate utilization in Red Canyon Creek, we also found evidence for biogeochemical transformations of nitrate in the hyporheic zone due to redox-related processes. In the hyporheic zones around the dams, we generally observed either a decrease in sulfate concentration or an increase in nitrate concentration, relative to stream water (Figure 6). Fanelli and Lautz (2008) found that dam structures in Red Canyon Creek generate anoxic patches in the hyporheic zone where bacterial (dissimilatory) sulfate reduction occurs and oxic patches where N-mineralization and N-nitrification occur. Nitrogen-containing chemical species are strongly influenced by oxygen availability. The hyporheic zone upstream of the man-made dam showed nitrate concentrations slightly less than those in stream water suggesting the potential of nitrate loss by dissimilatory reduction (Duff and Triska, 2000). In contrast to the upstream hyporheic zone, nitrate concentrations downstream of the man-made dam showed substantial increases in the hyporheic zone above stream water concentrations. Two distinct patterns emerge, nitrate production downstream and bacterial (dissimilatory) sulfate reduction upstream of the dam (Figure 6).

Patterns in nitrate concentration are likely coupled with processes that affect ammonium concentrations (i.e. mineralization and nitrification) (Fanelli and Lautz, 2008). Generally, nitrate and ammonium show opposing concentration patterns in the hyporheic zone, due primarily to the level of dissolved oxygen indicating the redox conditions in the hyporheic zone (Figure 7). Zones of high nitrate, low ammonium and high  $d\text{O}_2$  were found downstream of the dam, whereas upstream of the dam the hyporheic zone had low nitrate, high ammonium and low  $d\text{O}_2$  (Figure 7).

In previous work, we have measured rates of water flux into the hyporheic zone upstream of the man-made log dam that are relatively low (averaging  $1.8\ \text{cm day}^{-1}$ ), limiting the rate of oxygen replenishment from the overlying stream water (Fanelli and Lautz, 2008). We also see evidence for a low flux of stream water into the hyporheic zone from the streambed based on the  $\delta^{15}\text{N}$  values in this study. Upstream of the man-made dam, little change in  $\delta^{15}\text{N}$  values occurred from Day 1 to Day 3 (Figure 8) indicating that little isotopically labelled

nitrate was transported from the stream water above the sediment into the hyporheic zone.

Fanelli and Lautz (2008) observed significantly higher water flux through the downstream hyporheic zone (averaging  $12.4 \text{ cm day}^{-1}$ ) versus upstream around the man-made dam. We see evidence of this larger flux of stream water above the sediment into the hyporheic zone downstream of the dam from the hyporheic zone  $\delta^{15}\text{N}$  values. Day 2 increases in  $\delta^{15}\text{N}$  values were much greater downstream of the man-made dam compared to any of the other hyporheic zone locations (Figure 8).  $\delta^{15}\text{N}$  values decreased on Day 3 relative to Day 2, returning to near background levels. The patterns in  $\delta^{15}\text{N}$  values downstream of the man-made dam indicate much more rapid exchange of surface water with hyporheic sediments downstream of the dam. Coarse grained stream bed sediments in the riffle downstream of the man-made dam allow stream water to rapidly enter the hyporheic zone, replenishing oxygen to the sediments and hence facilitating the formation of nitrate and explaining the absence of denitrification (Fanelli and Lautz, 2008).

These upstream versus downstream patterns in N dynamics were most pronounced in the hyporheic zone surrounding the man-made dam that had been in place for over 15 years (Fanelli and Lautz, 2008). These patterns were less pronounced in the hyporheic zone surrounding the beaver dam because it is a less-developed geomorphic feature being less than 1-year old. Although the man-made dam was an area of relatively high hyporheic exchange compared to the beaver dam in this study, there was only a moderate connection between the stream water and hyporheic pore water. The area of highest hyporheic exchange, downstream of the man-made dam, had a nitrate  $\delta^{15}\text{N}_{\text{nitrate}}$  value of  $+392\%$  during Day 2 in Reach A. This level of  $^{15}\text{N}$  enrichment was approximately four times lower than the level of enrichment seen in the stream water nitrate in Reach A. Elsewhere, around the beaver dam and upstream of the man-made dam, the percent surface water contributions into the hyporheic zone were much lower. Redox patterns in the hyporheic zone show mechanisms by which nitrate can be taken up and returned to the water column (i.e. turned over). These hyporheic zone mechanisms are complimentary to the transformations of N by autotrophs in the water column.

#### Nitrate uptake and metabolism: intersite comparisons

Nutrient uptake parameters ( $S_w$  and  $S_{w,\text{net}}$ ) and stream discharge ( $Q$ ) were compared with results from 10 other nitrate addition studies (Valett *et al.*, 1996, 1997; Marti *et al.*, 1997; Haggard *et al.*, 2001; Thomas *et al.*, 2003; Bohlke *et al.*, 2004; Grimm *et al.*, 2005; Lautz and Siegel, 2007). For this study, the  $S_w$  values were generally within the range of values in other studies. However, the  $S_w$  values were longer than 75% of those in the other studies (Figure 10) suggesting a relatively slow processing of nitrate at Red Canyon Creek. Perhaps, this low processing rate at Red Canyon Creek is due to the relatively low nutrient demand and subsequently

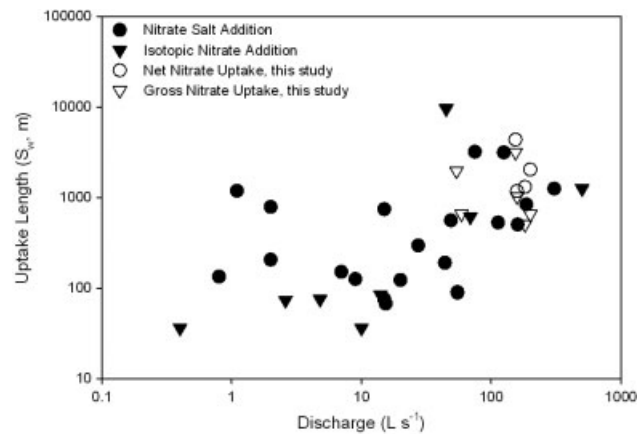


Figure 10. Stream discharge versus nitrate uptake or spiralling length for this study and other previous studies (Valett *et al.*, 1996; Valett *et al.*, 1997; Marti *et al.*, 1997; Haggard *et al.*, 2001; Thomas *et al.*, 2003; Bohlke *et al.*, 2004; Grimm *et al.*, 2005; Lautz and Siegel, 2007). Data is grouped by uptake length calculation method

lower primary productivity compared to other streams. In general,  $S_w$  increased with discharge over the range of all the studies (Figure 10).

The variation in nutrient uptake versus discharge reflects the importance of other parameters in influencing the uptake length, including differences among streams in the relative importance of autotrophic and heterotrophic processes. There is no clear relationship between uptake length and discharge when discharge rates are lower than approximately  $30 \text{ l s}^{-1}$  and uptake lengths derived from salt addition experiments are generally higher than those derived from isotopically labelled nitrate additions (Figure 10). For discharge rates greater than approximately  $100 \text{ l s}^{-1}$ ,  $S_w$  is generally larger than for lower discharge rates. These patterns in  $S_w$  are likely due to increases in stream water nitrate concentrations to levels well above ambient conditions during nitrate salt addition experiments. In contrast to nitrate salt addition tests,  $^{15}\text{N}$  tracer addition test results show lower  $S_w$  at lower stream discharges. However,  $S_w$  values from  $^{15}\text{N}$  tracer injection studies were comparable to chemical nitrate addition tests at high discharge. During  $^{15}\text{N}$  injection tests, stream water nitrate concentrations are not substantially altered and nitrate uptake mechanisms can be studied under ambient conditions, reducing the effects of experimental artefacts resulting in overestimates of nitrate uptake lengths.

We compared rates of reach-level GPP and ER with  $\text{NO}_3^-$  uptake velocity ( $V_f$ ;  $\text{m min}^{-1}$ ), where  $V_f = \frac{Q}{w \cdot S_w}$  ( $Q$  = reach discharge in  $\text{m}^3 \text{ min}^{-1}$  and  $w$  = approximate reach width in m), to a comparison of metabolism and  $V_f$  for 11 streams in Grand Teton National Park, Wyoming (Hall and Tank, 2003). There was a strong positive relationship between GPP and daytime  $V_f$  for all three Red Canyon Creek reaches and the other Wyoming streams; the relationship between ER and night-time  $V_f$  (we compared with night-time  $V_f$  because ER was calculated from night-time  $\text{O}_2$  consumption) was also significant for the Red Canyon Creek reaches (Figure 11). Similar to results in Hall and Tank (2003) and Hall *et al.* (2009a), GPP

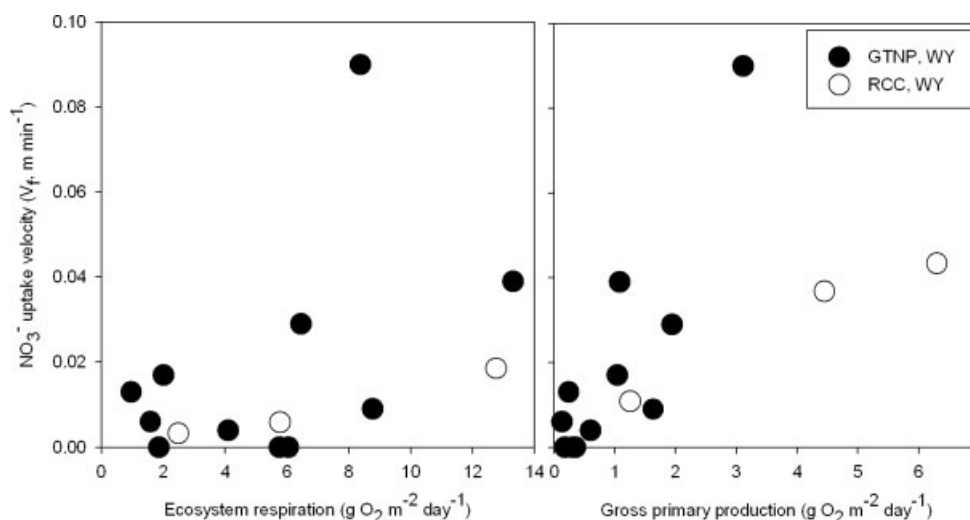


Figure 11. A comparison of metabolism (ER and GPP) and  $\text{NO}_3^-$  uptake velocity ( $V_f$ ) for three reaches of Red Canyon Creek (RCC, white circles), WY (via  $^{15}\text{N}-\text{NO}_3^-$  additions; this study) and 11 stream reaches in Grand Teton National Park (GTNP, black circles), WY (via  $\text{NO}_3^-$  additions; Hall and Tank, 2003). Because ER was calculated at night and GPP was calculated during the day, we compared rates of ER and GPP to night and day  $V_f$ , respectively. The regression equations for relationships between  $V_f$  and metabolism in the three Red Canyon Creek reaches were  $V_{f,\text{night}} = 0.0015 \text{ ER} + 0.0015$  ( $R^2 = 0.98$ ) and  $V_{f,\text{day}} = 0.0066 \text{ GPP} + 0.0038$  ( $R^2 = 0.97$ )

was the best predictor for changes in Red Canyon Creek daytime  $V_f$  ( $R^2 = 0.98$ ). The slope of GPP versus daytime  $V_f$  for Red Canyon Creek reaches was lower than for other Wyoming streams (Hall and Tank, 2003), but  $\text{NO}_3^-$  (instead of  $^{15}\text{N}-\text{NO}_3^-$ ) additions used by Hall and Tank may have overestimated  $\text{NO}_3^-$  uptake (Mulholland *et al.*, 2002) and/or deeper Red Canyon Creek reaches could have a lower N-removal efficiency than shallower streams.

## CONCLUSIONS

Background nitrate chemistry in stream water and  $^{15}\text{N}_{\text{nitrate}}$  stream addition tracer tests were used to derive  $S_w$  and  $S_{w,\text{net}}$  values for day and night in a third-order Rocky Mountain stream. Daytime gross nitrate uptake ( $S_w$ ) and net nitrate uptake ( $S_{w,\text{net}}$ ) lengths were generally shorter than night-time uptake lengths likely due to increased levels of photosynthetic activity and subsequent uptake and removal of nitrate from the water during the day. Such diurnal changes in uptake suggest autotrophic processes in the water column are primarily responsible for nitrate loss in Red Canyon Creek.

In-stream features, such as debris dams, caused substantial changes in stream water geochemistry as the stream water was diverted into the biologically and chemically reactive hyporheic zone. Denitrification in anoxic zones and mineralization/nitrification in oxic zones around the dams served to amplify the variability in geochemical conditions generally found in natural pool and riffle sequences. Highly oxic and anoxic zones in the streambed appeared to develop over multiple years around more permanent structures in the system, providing a mechanism by which N cycling can be enhanced in the hyporheic zone, increasing the potential for denitrification and enhancing overall uptake of nitrate in the stream system.

The obtained results on N dynamics in Rocky Mountain streams such as Red Canyon Creek have important biogeochemical and ecological implications (Earl *et al.*, 2006; Hall *et al.*, 2009b). Large increases in inorganic N have the potential to shift historically N-limited ecosystems to more N-saturated conditions, which may translate to greater inorganic N in downstream rivers (Fenn *et al.*, 2003a,b; Burns, 2004). Relatively pristine Rocky Mountain streams have higher streambed complexity and thus greater transient storage than other anthropogenically altered streams, which may correspond to greater N removal and transformation (Gooseff *et al.*, 2007; Hall *et al.*, 2009a). The results of this study help to put into context the importance of nitrogen removal and transformation in Rocky Mountain headwater streams and how these streams may react to increased inputs of inorganic N. If inputs of inorganic N continue to increase, knowing the biogeochemical response of these streams is critical.

## ACKNOWLEDGEMENTS

We thank The Nature Conservancy of Wyoming for access to the field site. We also thank Pat McHale, David Lyons, Lisa Kurian and Elias Anoszko for help with field work and laboratory analyses. We thank Pat Mulholland for advice and assistance with analytical issues related to this study. This work was made possible by funding from the National Science Foundation (EAR 0450317).

## REFERENCES

- Alexander RB, Smith RA, Schwarz GE. 2000. Effect of stream channel size on the delivery of nitrogen to the Gulf of Mexico. *Nature* **403**: 758–761.
- Bohlke JK, Harvey JW, Voytek MA. 2004. Reach-scale isotope tracer experiment to quantify denitrification and related processes in a nitrate-rich stream, midcontinent United States. *Limnology and Oceanography* **49**: 821–838.

- Burns DA. 1998. Retention of  $\text{NO}_3^-$  in an upland stream environment: a mass balance approach. *Biogeochemistry* **40**: 73–96.
- Burns DA. 2004. The effects of atmospheric nitrogen deposition in the Rocky Mountains of Colorado and southern Wyoming, USA—a critical review. *Environmental Pollution* **127**: 257–269. DOI: 10.1016/S0269-7491(03)00264-1.
- Cole JJ, Caraco NF. 1998. Atmospheric exchange of carbon dioxide in a low-wind oligotrophic lake measured by the addition of  $\text{SF}_6$ . *Limnology and Oceanography* **43**: 647–656.
- Duff JH, Triska FJ. 2000. Nitrogen biogeochemistry and surface-subsurface exchange in streams. In *Streams and ground waters*, Jones JB, Mulholland PJ (eds). Academic Press: San Diego, California.
- Earl SR, Valett HM, Webster JR. 2006. Nitrogen saturation in stream ecosystems. *Ecology* **87**: 3140–3151.
- Ensign SH, Doyle MW. 2006. Nutrient spiraling in streams and river networks. *Journal of Geophysical Research-Biogeosciences* **111**: G04009; DOI:10.1029/2005JG000114.
- Fanelli RM, Lautz LK. 2008. Patterns of water, heat and solute flux through the streambeds around small dams. *Ground Water* **46**: 671–687.
- Fellows CS, Valett HM, Dahm CN, Mulholland PJ, Thomas SA. 2006. Coupling nutrient uptake and energy flow in headwater streams. *Ecosystems* **9**: 788–804. DOI: 10.1007/S10021-006-0005-5.
- Fenn ME, Baron JS, Allen EB, Rueth HM, Nydick KR, Geiser L, Bowman WD, Sickman JO, Meixner T, Johnson DW, Neitlich P. 2003a. Ecological effects of nitrogen deposition in the western United States. *Bioscience* **53**: 404–420.
- Fenn ME, Haeuber R, Tonnesen GS, Baron JS, Grossman-Clarke S, Hope D, Jaffe DA, Copeland S, Geiser L, Rueth HM, Sickman JO. 2003b. Nitrogen emissions, deposition, and monitoring in the western United States. *Bioscience* **53**: 391–403.
- Galloway JN, Cowling EB. 2002. Reactive nitrogen and the World: 200 years of change. *Ambio* **31**: 64–71.
- Gooseff MN, Hall RO, Tank JL. 2007. Relating transient storage to channel complexity in streams of varying land use in Jackson Hole, Wyoming. *Water Resources Research* **43**: W01417. DOI: 10.1029/2005WR004626.
- Grimm NB, Sheibley RW, Crenshaw CL, Dahm CN, Roach WJ, Zeglin LH. 2005. N retention and transformation in urban streams. *Journal of the North American Benthological Society* **24**: 626–642.
- Haggard BE, Storm DE, Tejral RD, Popova YA, Keyworth VG, Stanley EH. 2001. Stream nutrient retention in three northeastern Oklahoma agricultural catchments. *Transactions of the ASAE* **44**: 597–605.
- Hall RO, Tank JL. 2003. Ecosystem metabolism controls nitrogen uptake in streams in Grand Teton National Park, Wyoming. *Limnology and Oceanography* **48**: 1120–1128.
- Hall RO, Thomas S, Gaiser EE. 2007. Measuring primary production and respiration in freshwater ecosystems. In *Principles and standards for measuring primary production*, Fahey TJ, Knapp AK (eds). Oxford Press: Oxford; 175–203.
- Hall RO, Baker MA, Arp CD, Koch BJ. 2009a. Hydrologic control of nitrogen removal, storage, and export in a mountain stream. *Limnology and Oceanography* **54**: 2128–2142.
- Hall RO, Tank JL, Sobota DJ, Mulholland PJ, O'Brien JM, Dodds WK, Webster JR, Valett HM, Poole GC, Peterson BJ, Meyer JL, McDowell WH, Johnson SL, Hamilton SK, Grimm NB, Gregory SV, Dahm CN, Cooper LW, Ashkenas LR, Thomas SM, Sheibley RW, Potter JD, Niederlehner BR, Johnson LT, Helton AM, Crenshaw CM, Burgin AJ, Bernot MJ, Beaulieu JJ, Arango CP. 2009b. Nitrate removal in stream ecosystems measured by N-15 addition experiments: total uptake. *Limnology and Oceanography* **54**: 653–665.
- Jin L, Siegel DI, Lautz LK, Mitchell MJ, Dahm DE, Mayer B. 2010. Calcite precipitation driven by the common ion effect during groundwater-surface water mixing: a potentially common process in streams with geologic settings containing gypsum. *Geological Society of America Bulletin* **122**: 1027–1038.
- Lautz LK, Siegel DI. 2006. Modeling surface and ground water mixing in the hyporheic zone using MODFLOW and MT3D. *Advances in Water Resources* **29**: 1618–1633.
- Lautz LK, Siegel DI. 2007. The effect of transient storage on nitrate uptake lengths in streams: an inter-site comparison. *Hydrological Processes* **21**: 3533–3548.
- Lautz LK, Siegel DI, Bauer RL. 2006. Impact of debris dams on hyporheic interaction along a semi-arid stream. *Hydrological Processes* **20**: 183–196.
- Marti E, Grimm NB, Fisher SG. 1997. Pre- and post-flood retention efficiency of nitrogen in a Sonoran desert stream. *Journal of the North American Benthological Society* **16**: 805–819.
- Mulholland PJ, DeAngelis DL. 2000. Surface-subsurface exchange and nutrient spiraling. In *Streams and Ground Waters*, Jones JB, Mulholland PJ (eds). Academic Press: San Diego, CA; 149–168.
- Mulholland PJ, Tank JL, Webster JR, Bowden WB, Dodds WK, Gregory SV, Grimm NB, Hamilton SK, Johnson SL, Marti E, McDowell WH, Merriam JL, Meyer JL, Peterson BJ, Valett HM, Wollheim WM. 2002. Can uptake length in streams be determined by nutrient addition experiments?: Results from an interbiome comparison study. *Journal of the North American Benthological Society* **21**: 544–560.
- Mulholland PJ, Thomas SA, Valett HM, Webb JA, Beaulieu J. 2006. Effect of light on  $\text{NO}_3^-$  uptake in small forested streams: diurnal and day-to-day variations. *Journal of the North American Benthological Society* **25**: 583–595.
- Mulholland PJ, Helton AM, Poole GC, Hall RO, Hamilton SK, Peterson BJ, Tank JL, Ashkenas LR, Cooper LW, Dahm CN, Dodds WK, Findlay SEG, Gregory SV, Grimm NB, Johnson SL, McDowell WH, Meyer JL, Valett HM, Webster JR, Arango CP, Beaulieu JJ, Bernot MJ, Burgin AJ, Crenshaw CL, Johnson LT, Niederlehner BR, O'Brien JM, Potter JD, Sheibley RW, Sobota DJ, Thomas SM. 2008. Stream denitrification across biomes and its response to anthropogenic nitrate loading. *Nature* **452**: 202–U246. DOI: 10.1038/Nature06686.
- Newbold J, Elwood J, O'Neill R, Winkle WV. 1981. Measuring nutrient spiraling in streams. *Canadian Journal of Fisheries and Aquatic Science* **38**: 860–863.
- Odom HT. 1956. Primary production in flowing waters. *Limnology and Oceanography* **1**: 102–117.
- Payn RA, Webster JR, Mulholland PJ, Valett HM, Dodds WK. 2005. Estimation of stream nutrient uptake from nutrient addition experiments. *Limnology and Oceanography: Methods* **3**: 174–182.
- Peterson BJ, Wollheim WM, Mulholland PJ, Webster JR, Meyer JL, Tank JL, Marti E, Bowden WB, Valett HM, Hershey AE, McDowell WH, Dodds WK, Hamilton SK, Gregory S, Morrall DD. 2001. Control of nitrogen export from watersheds by headwater streams. *Science* **292**: 86–90.
- Rockstrom J, Steffen W, Noone K, Persson A, Chapin FS, Lambin EF, Lenton TM, Scheffer M, Folke C, Schellnhuber HJ, Nykvist B, de Wit CA, Hughes T, van der Leeuw S, Rodhe H, Sorlin S, Snyder PK, Costanza R, Svedin U, Falkenmark M, Karlberg L, Corell RW, Fabry VJ, Hansen J, Walker B, Liverman D, Richardson K, Crutzen P, Foley JA. 2009. A safe operating space for humanity. *Nature* **461**: 472–475. DOI: 10.1038/461472a.
- Schlesinger WH. 2009. On the fate of anthropogenic nitrogen. *Proceedings of the National Academy of Sciences of the United States of America* **106**: 203–208.
- Seitzinger SP. 1988. Denitrification in fresh-water and coastal marine ecosystems—ecological and geochemical significance. *Limnology and Oceanography* **33**: 702–724.
- Seitzinger SP, Styles RV, Boyer EW, Alexander RB, Billen G, Howarth RW, Mayer B, Van Breemen N. 2002. Nitrogen retention in rivers: model development and application to watersheds in the northeastern USA. *Biogeochemistry* **57**: 199–237.
- Sigman DM, Casciotti KL, Andreani M, Barford C, Galanter M, Bohlke JK. 2001. A bacterial method for the nitrogen isotopic analysis of nitrate in seawater and freshwater. *Analytical Chemistry* **73**: 4145–4153.
- Stream Solute Workshop. 1990. Concepts and methods for assessing solute dynamics in stream ecosystems. *Journal of the North American Benthological Society* **9**: 95–119.
- Thomas SA, Valett HM, Webster JR, Mulholland PJ. 2003. A regression approach to estimating reactive solute uptake in advective and transient storage zones of stream ecosystems. *Advances in Water Resources* **26**: 965–976.
- Valett HM, Morrice JA, Dahm CN, Campana ME. 1996. Parent lithology, surface-groundwater exchange, and nitrate retention in headwater streams. *Limnology and Oceanography* **41**: 333–345.
- Valett HM, Dahm CN, Campana ME, Morrice JA, Baker MA, Fellows CS. 1997. Hydrologic influences on groundwater-surface water ecotones: heterogeneity in nutrient composition and retention. *Journal of the North American Benthological Society* **16**: 239–247.
- Wanninkhof R. 1992. Relationship between wind-speed and gas-exchange over the ocean. *Journal of Geophysical Research-Oceans* **97**: 7373–7382.
- Wanninkhof R, Mulholland PJ, Elwood JW. 1990. Gas-exchange rates for a 1st-order stream determined with deliberate and natural tracers. *Water Resources Research* **26**: 1621–1630.
- Williams MW, Hood E, Caine N. 2001. Role of organic nitrogen in the nitrogen cycle of a high-elevation catchment, Colorado front range. *Water Resources Research* **37**: 2569–2581.